

# RSC Advances



This is an *Accepted Manuscript*, which has been through the Royal Society of Chemistry peer review process and has been accepted for publication.

*Accepted Manuscripts* are published online shortly after acceptance, before technical editing, formatting and proof reading. Using this free service, authors can make their results available to the community, in citable form, before we publish the edited article. This *Accepted Manuscript* will be replaced by the edited, formatted and paginated article as soon as this is available.

You can find more information about *Accepted Manuscripts* in the [Information for Authors](#).

Please note that technical editing may introduce minor changes to the text and/or graphics, which may alter content. The journal's standard [Terms & Conditions](#) and the [Ethical guidelines](#) still apply. In no event shall the Royal Society of Chemistry be held responsible for any errors or omissions in this *Accepted Manuscript* or any consequences arising from the use of any information it contains.

## COMMUNICATION

## Hydrogen evolution inhibition with diethylenetriamine modification of activated carbon for lead-acid battery

Cite this: DOI: 10.1039/x0xx00000x

Bo Hong, Xiaoying Yu, Liangxing Jiang\*, Haitao Xue, Fangyang Liu\*, Jie Li, Yexiang Liu

Received 00th May 2014,  
Accepted 00th January 2012

DOI: 10.1039/x0xx00000x

www.rsc.org/

**A novel idea to inhibit hydrogen evolution of activated carbon (AC) application in lead-acid battery has been presented in this paper. Nitrogen groups-enriched AC (NAC, mainly exists as pyrrole N) was prepared. Electrochemical measurements demonstrate that the hydrogen evolution reaction (HER) is markedly inhibited as the HER impedance increased significantly. What's more, the specific capacitance value of NAC is 142.5% higher than AC since working window extended. The use of NAC, instead of AC in UltraBattery, can inhibit the hydrogen evolution, improve battery's charge acceptance and charge retention ability.**

Conventional lead-acid batteries suffer from a progressive build-up of "hard" lead sulfate and are difficult to recharge under high-rate partial-state-of-charge (HRPSoC) conditions. To address this problem, more attention has been focused on improving the cycle ability of the Valve-Regulated Lead-Acid Battery (VRLA) under HRPSoC duty. Some researchers observed that carbon materials added to the negative plate of lead-acid battery could suppress the sulphation phenomenon efficiently, and these new batteries were named lead-carbon battery<sup>1-3</sup> or UltraBattery<sup>4-6</sup>. These recent discoveries have excited great interest among battery producers. However, under the cathodic working conditions of lead-acid battery (-0.86~-1.36V vs. Hg/Hg<sub>2</sub>SO<sub>4</sub>, 5 mol·L<sup>-1</sup> sulfuric acid), the activated carbon (AC) will perform low capacity and serious hydrogen evolution reaction (HER)<sup>5,6</sup>. As a result, more gas will evolve at the end of charge and cause the thermal runaway<sup>7</sup> or even electrolyte dry-out of the battery. For the problem of HER, physical mixing or chemical depositing high HER overpotential metal impurities through occupying the reactive sites to inhibit the HER was opined to be an effective way<sup>8</sup>, but the inhibitory effect of HER was unstable as dopants were difficult to disperse evenly.

Usually, HER can occur through two separate pathways, the Volmer-Tafel or the Volmer-Heyrovsky mechanism<sup>9</sup>, both of which involve hydrogen intermediate adsorption and desorption on the electrode surface. "Volcano Plots", demonstrated by Trasatti<sup>10</sup>, Parsons<sup>11</sup> and Nørskov<sup>12</sup>, relates the exchange current density of the elements for the HER in acid to a calculated metal-hydrogen (M-H) bond strength derived by Krishtalik<sup>13</sup>. Very generally, these volcano relations state that materials with too low or too high bond strength

of M-H result in slow kinetics for HER—Pb or Al for example. Based on this principle, we considered that AC doped with heteroatoms (N, P, B, S) in the graphene ring must be a potential method for HER inhibition. Since the electronic properties of carbon materials were theoretically predicted to change by the presence of the heteroatoms due to their different electronegativity from carbon. Through controlling proper heterocyclic structure and content, AC with extreme (very low or very high) bond strength to hydrogen would be obtained, and then results in high hydrogen evolution resistance.

Activated carbon from Shanghai Kuraray Company was used as the original carbon material. Original AC (0.5 g) was slowly added into a mixture of 75 mL diethylenetriamine and 25 mL anhydrous ethyl alcohol. Followed by refluxing at 80 °C for 4 h, the diethylenetriamine-treated AC was filtered and washed thoroughly with deionized water. After being dried at 80 °C for 10 h, the product was obtained and named as Nitrided AC (NAC).

K-Alpha 1063 X-ray photoelectron spectrometer was performed for exploring the content and configuration of nitrogen doped AC. The full range XPS analysis (Fig. 1a, red curve) of NAC clearly shows the presence of nitrogen (N), carbon (C) and oxygen (O) with an atomic percentage of 87.35%, 4.99% and 7.66%, respectively. However, there is almost no nitrogen observed in the original AC. The XPS spectra of N1s core level were fitted into three peaks with the Shirley-type background and 30% of Lorentzian to Gaussian peak shape (Fig. 1b). The fitting of N1s peaks gives the following binding energies (BE): 398.14 eV for pyridine-N, 399.98 eV usually for pyrrole N, and 402.40 eV for nitrogen substituents in aromatic graphene structures (graphite N, as shown in Fig. 1d)<sup>14-16</sup>. Raman spectroscopy measurements were performed with a LabRAM HR800 Raman spectrometer. As shown in Fig. 1c, both ACs have similar Raman scattering patterns. The intensity ratios of  $I_D/I_G$  are 0.972 and 1.017 for original AC and NAC, respectively, which means a little more chemical and/or physical defects the NAC has<sup>17</sup>. This is inevitable as the embedment of nitrogen heteroatoms in aromatic rings. Fig. 1e and Fig. 1f provides the SEM images of original AC and NAC. It can be seen that both samples are almost the same that mainly consist of large particles (2-10 μm) and plentiful small particles (less than 2 μm). Raman and SEM

results prove that no serious structure damage of AC occurred in this modification process.

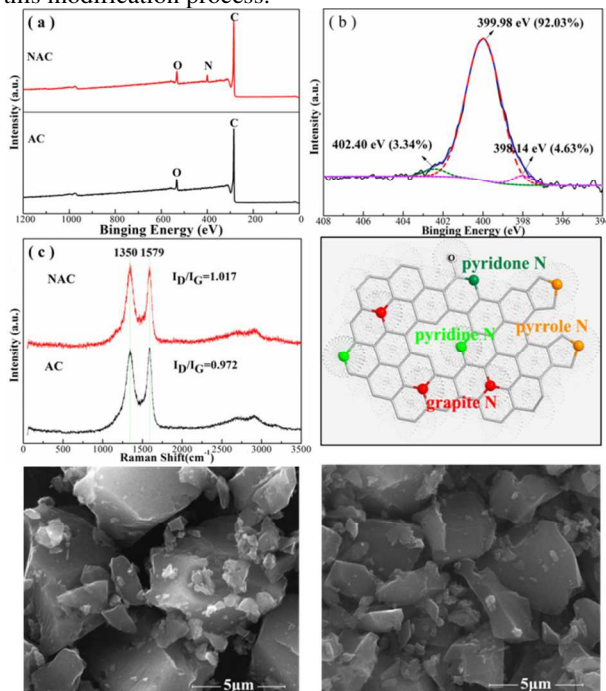


**Fig. 1.** (a) XPS valence band spectra for NAC and original AC; (b) N1s XPS spectra for NAC; (c) Raman spectra for NAC and original AC; (d) Schematic illustration of N-doped AC; (e) SEM images of original AC; (f) SEM images of NAC.

All electrochemical experiments were performed in a three-electrode system by a Princeton 2273 electrochemical working station. The mercury/mercurous sulphate reference electrode ( $\text{Hg}/\text{HgSO}_4$ ) was used as the reference electrode. The electrolyte was  $5 \text{ mol}\cdot\text{L}^{-1}$  sulfuric acid solution.

Linear Sweep Voltammetry (LSV) curves of both samples are presented in Fig. 2a. The hydrogen evolution current for NAC is  $-1.03 \text{ A}\cdot\text{g}^{-1}$  under  $-1.36 \text{ V}$ , which is only 12% of the original AC, indicating that the HER is significantly inhibited in NAC electrodes. Furthermore, the onset potential of hydrogen evolution is  $-1.22 \text{ V}$  for NAC but  $-1.04 \text{ V}$  for AC. When potential lower than these values, the hydrogen evolution current exponential increases with the potential negatively shifted. This means that during early stages of discharge in lead-acid battery, hydrogen evolution rather than discharge may occur on AC. Toward the end of charge, AC will also cause serious hydrogen evolution because its potential is shifted to a more negative value. It results that original AC cannot act as an efficient buffer during high-rate discharge and charge progress. However, NAC can overcome this defect effectively.

For the above reason, original AC often shows very low capacity and narrow charge and discharge potential window in  $5 \text{ M H}_2\text{SO}_4$  solution under the cathodic working conditions of lead-acid battery in spite of the relatively high BET surface. As shown in Fig. 2b, NAC exhibits a better capacity performance with the specific capacitance value of  $28.52 \text{ F}\cdot\text{g}^{-1}$ , which is 142.5% higher than that of original AC ( $11.76 \text{ F}\cdot\text{g}^{-1}$ ), and its charge separation and neutralization window was extended to the whole potential region.

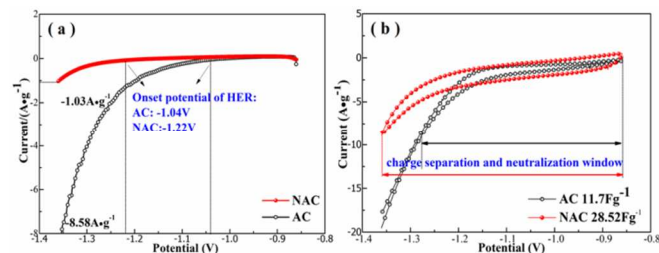


**Fig. 2.** (a) LSV curves of AC and NAC (scan range:  $-0.86 \text{ V}$  to  $-1.36 \text{ V}$ ; scan rate:  $1.0 \text{ mV}\cdot\text{s}^{-1}$ ) (b) CV curves of AC and NAC (scan range:  $-0.86 \text{ V}$  to  $1.36 \text{ V}$ , scan rate:  $10 \text{ mV}\cdot\text{s}^{-1}$ ).

EIS spectra of AC and NAC were collected under various potentials. As shown in Fig. 3a and Fig. 3b, the spectra were mainly composed of one small arc in the high frequency region and one large capacitive arc in the low frequency region. The small capacitive arc was observed to be independent of potential and considered as a description of the resistive/capacitive behavior associated with the charge transfer processes. The large capacitive arc in the low frequency region, decreased exponentially with the decrease of applied potential, was related to the adsorption of intermediates<sup>18</sup>.

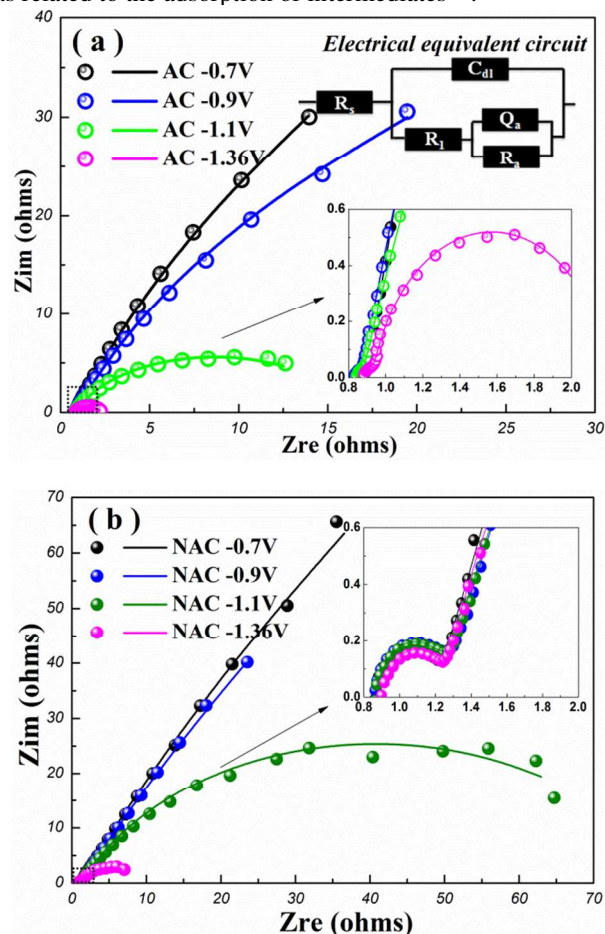


**Fig. 3.** Nyquist spectra obtained on (a) AC and (b) NAC at various potentials. Electrolyte:  $5 \text{ M H}_2\text{SO}_4$ , Temperature:  $25 \text{ }^\circ\text{C}$

The equivalent electrical circuit (EEC) proposed by Armstrong and Henderson<sup>18, 19</sup> to model the impedance of HER is shown in the insert map of Fig. 3a. In which  $R_s$  is the sum of electrode resistance and solution resistance;  $C_{dl}$  is the

double-layer capacitance,  $R_1$  denotes the charge transfer resistance;  $R_a$  and  $C_a$  are equivalent resistance and pseudo-capacitance associated with the adsorption of intermediates, respectively. Constant Phase Elements ( $Q_a$ ) were used to replace the capacitors ( $C_a$ ) in the simulation.

Parameter values of EEC obtained by fitting the EIS experimental data of the investigated electrodes are given in table 1. It was found that  $R_a$  is much higher than  $R_1$ , which indicates that the rate-determining step of HER on AC surface is the adsorption step of intermediates. The  $R_a$  value of NAC is much higher than that of AC, which means that AC doped by nitrogen can increase the adsorption resistance of hydrogen and inhibit the hydrogen evolution. Accordingly, the  $C_{dl}$  of NAC is much lower than original AC. Due to the stronger electronegativity of nitrogen atom than that of carbon, nitrogen atoms doped in carbon matrix can attract the electrons of the neighboring or further carbon atoms, making them electron deficient. Thus, the adsorption of hydrogen atoms on NAC surface may be inhibited since it is likely to be stabilized through sharing a couple of electrons with carbon.

**Table 1** Fit parameters for AC and NAC in 5 M  $H_2SO_4$  under different potentials

	Potential (V)	$R_s$ ( $\Omega$ )	$Q_a$ (S·sec <sup>n</sup> )	$n$	$R_a$ ( $\Omega$ )	$C_{dl}$ (F·cm <sup>-2</sup> )	$R_1$ ( $\Omega$ )
AC	-0.7	0.884	0.022	0.8045	234.2	2.8E-3	0.03
	-0.9	0.837	0.026	0.797	134.8	1.4E-3	0.04
	-1.1	0.847	0.020	0.785	15.6	8.5E-4	0.05
	-1.36	0.886	0.012	0.803	1.2	7.7E-4	0.07
NAC	-0.7	0.8702	0.0298	0.7344	727	1.3E-4	0.35
	-0.9	0.8709	0.0294	0.7199	619	1.4E-4	0.39
	-1.1	0.8786	0.0237	0.729	79.1	1.3E-4	0.38
	-1.36	0.9194	0.016	0.7978	7.8	1.2E-4	0.34

In this paper, ACUB (UltraBattery with one Pb negative plate, one AC capacitive negative plate, and one  $PbO_2$  positive plate between them) and NACUB (The same structure with ACUB while the capacitive negative plate was changed to NAC) were assembled. All negative plates have a size of 4.0 cm × 6.8 cm (height×width) and geometric area of 27.2 cm<sup>2</sup>. The current distribution between the Pb negative plate and capacitor negative plate in a charge-discharge cycle were tested (as shown in Fig. 4), the regular lead-acid battery (LB) was used as the reference.

At charge steps, AC negative plate takes most of the charge current in ACUB despite its capacity is much lower than Pb negative plate. This is because that hydrogen evolution potential of AC is very low and HER wasted a large amount of energy. For this reason, the charging acceptance must decrease and the water loss will be exacerbated. Fortunately, this bad effect was inhibited obviously in NACUB. The NAC negative plate consumes little power and about 80% charging energy is accepted by Pb negative plate. This indicates that little charging energy is wasted and the decrease of charging acceptance is effectively relieved.

At standing step, AC negative plate is charged by Pb negative plate with an inner self-discharge current about 25~40 mA in the whole standing loop in ACUB. Besides, we can obviously observe the gas evolution from AC negative plate. This galvanic cell formed by Pb and AC plates inevitably do harm to the battery's charge retention ability. The inner self-discharge current is also observed in NACUB, but the value is significantly decreased to only 3 mA.

L.T. Lam<sup>5</sup> noted that the capacitor would enhance the power and lifespan of the lead-acid battery as it acts as a buffer in discharging and charging. But this behavior may be restrained by the properties of AC. During early stages of discharge, the current

mainly comes from the lead-acid negative plate and only little from the capacitor plate owing to its higher charge-neutralization potential. This inference is confirmed here, and it would be worse. In the ACUB, AC negative plate is not discharged rather charged by Pb negative plate during the early state of discharge. The AC negative plate only starts to discharge when the ACLB is brought to 60% SoC. Obviously, this is not the desirable condition. However, this problem is overcome by NAC and a large discharge current from capacitor electrode is observed at the beginning of discharge process. It indicates that NAC could act as a better buffer in discharging and charging process.

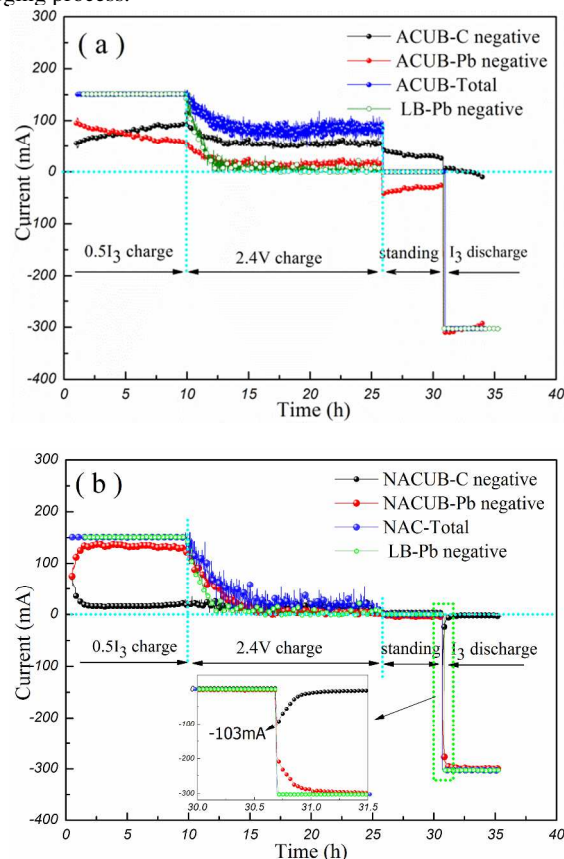


**Fig. 4.** Current distribution in Pb and C negative plates of (a) ACUB and (b) NACUB in a charge-discharge cycle. (Electrolyte: 5M  $H_2SO_4$ , Temperature: 25 °C)

## Conclusions

In this work, nitrogen groups-enriched activated carbon is prepared through diethylenetriamine modification. The nitrogen atoms added in the carbon material are mainly pyrrole N which are directly embedded in the graphene plane rings. Due to the stronger electronegativity of nitrogen atom than that of carbon, nitrogen atoms doped in carbon matrix can attract the electrons of the neighboring and/or further carbon atoms, making them electron deficient and then weakening the bond strength to hydrogen. For this reason, hydrogen adsorption step of HER is hindered and hydrogen evolution is great inhibited. In addition, the nitrogen groups-enriched activated carbon exhibits better

capacity performance and its charge separation and neutralization window was extended to the whole potential region of lead-acid battery. The use of NAC in UltraBattery can dramatically decrease the hydrogen evolution current, improve battery's charge acceptance and charge retention ability. In sum, the nitrogen groups-enriched activated carbon will be a prospective active electrode material for lead-acid battery, UltraBattery and lead-carbon battery.

### Notes and references

School of Metallurgy and Environment, Central South University, Changsha Hunan 410083, China

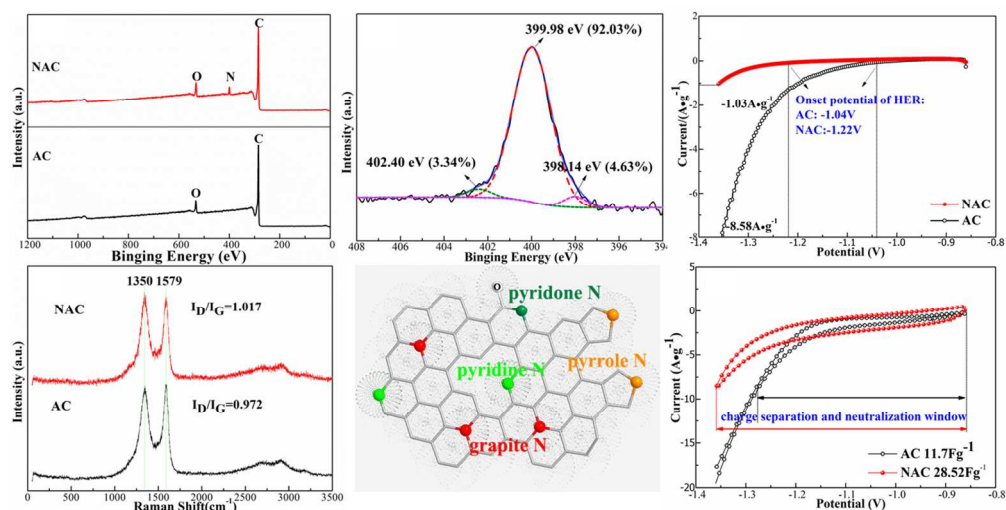
\*Corresponding author: Liangxing Jiang and Fangyang Liu

E-mail: lxjiang@csu.edu.cn and liufangyang@csu.edu.cn

Tel. and Fax: +86 731 88830649

This research was supported by the National Science & Technology Pillar Program of China (No. 2012BAA03B04), the Chinese National Natural Science Foundation (No. 51204208), the China Postdoctoral Science Foundation (No. 2013M540638, No. 2014T70788) and the Fundamental Research Funds for the Central Universities of Central South University (No. CX2012B049).

- 1 K. Nakamura, M. Shiomi, K. Takahashi, M. Tsubota, J. Power Sources, 1996, **59**, 153.
- 2 M. Calábek, K. Míčka, P. Křivák, P. Bača, J. Power Sources, 2006, **158**, 864.
- 3 D. Pavlov, T. Rogachev, P. Nikolov, G. Petkova, J. Power Sources, 2009, **191**, 58.
- 4 L.T. Lam, R. Louey, N.P. Haigh, O.V. Lim, D.G. Vella, C.G. Phyland, L.H. Vu, J. Furukawa, T. Takada, D. Monma, T. Kano, J. Power Sources, 2007, **174**, 16.
- 5 L.T. Lam, R. Louey, J. Power Sources, 2006, **158**, 1140.
- 6 J. Furukawa, T. Takada, D. Monma, L.T. Lam, J. Power Sources, 2010, **195**, 1241.
- 7 D. Pavlov, J. Power Sources, 1997, **64**, 131.
- 8 Y.F. Gao, Y.L. Song, D.L. Ren, Y.P. Wang, Journal of Inorganic Materials, 2013, **28**, 1301.
- 9 K. Mazloomi, C. Gomes. Renewable and Sustainable Energy Reviews, 2012, **16**, 3024.
- 10 S. Trasatti, J. Electroanal. Chem., 1972, **39**, 163.
- 11 R. Parsons, Transactions of the Faraday Society, 1958, **54**, 1053.
- 12 J.K. Nørskov, J. Rossmeisl, A. Logadottir, L. Lindqvist, et al, J. Phys. Chem. B, 2004, **108**, 17886.
- 13 Krishtalik, L. I. Russ. J. Phys. Chem., 1960, **34**, 53.
- 14 K. Jurewicz, K. Babel, A. Żiółkowski, H. Wachowska, Electrochimica Acta, 2003, **48**, 1491.
- 15 K.Y. Kang, B.I. Lee, J.S. Lee, Carbon, 2009, **47**, 1171.
- 16 M. Sankaran, B. Viswanathan, Carbon, 2006, **44**, 2816.
- 17 M.J. Matthews, M.A. Pimenta, G. Dresselhaus, M.S. et al, Physical Review B, 1999, **59**, 6585.
- 18 R.D. Armstrong, M. Henderson, J. Electroanal. Chem., 1972, **39**, 81.
- 19 A. Lasia, A. Rami, J. Electroanal. Chem., 1990, **294**, 123.



A novel idea to inhibit hydrogen evolution of AC application in lead-acid battery has been present in this communication. Nitrogen groups-enriched AC was prepared. Electrochemical measurements demonstrate that the hydrogen evolution reaction (HER) is markedly inhibited as the HER impedance increased significantly. What's more, the specific capacitance value of NAC is 142.5% higher than AC since working window extended. NAC instead of AC using in UltraBattery can decrease the hydrogen evolution, improve battery's charge acceptance and charge retention ability.

238x173mm (150 x 150 DPI)